Journal of Crystal Growth 312 (2010) 2631–2636

Contents lists available at ScienceDirect

Journal of Crystal Growth

journal homepage: www.elsevier.com/locate/jcrysgro

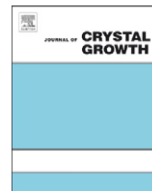

Hydride-assisted growth of GaN nanowires on Au/Si(0 0 1) via the reaction of Ga with NH_3 and H_2

Matthew Zervos [a,*], Andreas Othonos [b]

[a] Nanostructured Materials & Devices Laboratory, Department of Mechanical Engineering, Materials Science Group, University of Cyprus, Kalipoleos 75, 1678 Nicosia, P.O. Box 20573, Cyprus

[b] Research Centre of Ultrafast Science, Department of Physics, University of Cyprus, Kalipoleos 75, 1678 Nicosia, P.O. Box 20573, Cyprus

ARTICLE INFO

Article history:
Received 11 May 2010
Accepted 27 May 2010
Communicated by: K.W. Benz
Available online 2 June 2010

Keywords:
A1. Nanostructures
A1. Nanowires
A3. Hydride vapor phase epitaxy
B1. Nanomaterials
B1. Nitrides
B1. Oxides

ABSTRACT

High quality, straight GaN nanowires (NWs) with diameters of 50 nm and lengths up to 3 μm have been grown on Si(0 0 1) using Au as a catalyst and the direct reaction of Ga with NH_3 and N_2:H_2 at 900 °C. These exhibited intense, near band edge photoluminescence at 3.42 eV in comparison to GaN NWs with non-uniform diameters obtained under a flow of Ar:NH_3, which showed much weaker band edge emission due to strong non-radiative recombination. A significantly higher yield of β-Ga_2O_3 NWs with diameters of ≤50 nm and lengths up to 10 μm were obtained, however, via the reaction of Ga with residual O_2 under a flow of Ar alone. The growth of GaN NWs depends critically on the temperature, pressure and flows in decreasing order of importance but also the availability of reactive species of Ga and N. A growth mechanism is proposed whereby H_2 dissociates on the Au nanoparticles and reacts with Ga giving Ga_xH_y thereby promoting one-dimensional (1D) growth via its reaction with dissociated NH_3 near or at the top of the GaN NWs while suppressing at the same time the formation of an underlying amorphous layer. The higher yield and longer β-Ga_2O_3 NWs grow by the vapor liquid solid mechanism that occurs much more efficiently than nitridation.

© 2010 Elsevier B.V. All rights reserved.

1. Introduction

Group III-nitride (III-N) compound semiconductors such as GaN, InN and AlN have been investigated intensively over the past two decades in view of their successful application as electronic and optoelectronic devices [1–3]. In particular III-nitride semiconductors are attractive since their band-gaps vary between 0.7 eV in the case of InN [4] through 3.4 eV in GaN [5] up to 6.2 eV in AlN [6] allowing the band-gaps of $Al_xGa_{1-x}N$ [7] or $In_xGa_{1-x}N$ [8] to be tailored in between by varying x. Group III-nitride nanowires (NWs) have also been investigated in view of the up surging interest in nanostructured materials, nanoscale science and technology. More specifically InN [9], GaN [10] and AlN [11] NWs but also $In_xGa_{1-x}N$ NWs [12] have been grown and their transport and optical properties have been investigated. GaN NWs in particular have been grown by a variety of methods including metal organic chemical vapor deposition (MOCVD) [13] and molecular beam epitaxy (MBE) [14,15] but also via the direct nitridation of Ga with NH_3 [16–24]. In addition GaN NWs have been obtained by the reaction of Ga:GaN [25], Ga:SiO_2 [26] and Ga:GaN:CNT [27] with NH_3 but also at temperatures as low as 650 °C using Ga:CaF_2 [28] or $(CH_3COCHCOCH_3)_3Ga$ [29]. Finally it is worthwhile pointing out that GaN NWs have also been obtained via the nitridation of Ga_2O_3 [30–32]. Most of these GaN NWs have been grown via the direct reaction of Ga with NH_3 using Ar as a carrier gas between 900 and 1100 °C on a broad variety of substrates e.g. 6H–SiC [24] Al_2O_3 [26], $LaAlO_3$ [32], Si [27] using various catalysts such as $InCl_3$ [17], In, Fe [19], Ni [19], Au [21] and NiO [26]. The GaN NWs crystallise in the hexagonal wurtzite structure and their diameters typically vary between 10 and 50 nm. Nevertheless, despite this broad variety of investigations on GaN NWs there are still many issues pertaining to their growth and properties that need to be clarified and understood in order to improve their crystal quality and enable the fabrication of nanoscale devices.

Here we have carried out an investigation into the growth of GaN NWs on Au/Si(0 0 1) via the direct reaction of Ga with NH_3 using either Ar or N_2:H_2 as carrier gasses under different temperatures, pressures and gas flows. We find that the growth of GaN NWs on Au/Si(0 0 1) via the direct reaction of Ga with NH_3 is critically dependent on the vapor pressure of Ga over the Au/Si(0 0 1) surface that is dictated by the temperature, pressure and flows in decreasing order of importance.More importantly H_2 promotes the growth of straight GaN NWs and leads to an increase in the PL intensity via a reduction of the non-radiative recombination associated with surface and crystal structure

* Corresponding author. Tel.: +357 22892194; fax: +357 22892254.
E-mail address: zervos@ucy.ac.cy (M. Zervos).

0022-0248/$ - see front matter © 2010 Elsevier B.V. All rights reserved.
doi:10.1016/j.jcrysgro.2010.05.040

imperfections. A growth mechanism is proposed whereby H_2 dissociates at the Au nanoparticle sites and reacts with Ga giving Ga_xH_y thereby promoting one-dimensional (1D) growth via its reaction with dissociated NH_3 near the top of the GaN NWs while suppressing at the same time the formation of an underlying amorphous α-Ga rich oxynidtride layer obtained when using Ar.

2. Experimental method

GaN NWs were grown using an atmospheric pressure chemical vapor deposition (APCVD) reactor, which consists of four mass flow controllers (MFC's) and a 1″ horizontal quartz tube (QT) furnace, capable of reaching a maximum temperature of 1100 °C. In addition GaN NWs were grown at low pressures (LP) in which case the 1″ QT was fed from the MFC manifold on the upstream side via a needle valve and connected to a pump on the exhaust side. The pressure gauge (PG), on the other hand, was connected just after the needle valve on the upstream side to prevent its contamination by Ga. Upon installation, each 1″ QT was always heated to 900 °C at 30 °C/min and maintained at 900 °C for 15 min under a constant flow of 100 standard cubic centimetres per minute (sccms) of Ar after which it was allowed to cool down to room temperature (RT). For the growth of GaN NWs, 0.01–0.5 g of solid Ga fragments (Aldrich, 99.99%) stored below its melting point of 30 °C were cut, weighed and loaded in a quartz boat while square pieces of n^+ Si(0 0 1) ≈7 mm × 7 mm, coated with 0.5 nm of Au, were loaded at various distances from the Ga. The Au layer was deposited via sputtering using an Ar plasma under a pressure of $\approx 10^{-2}$ mBar. The boat was always loaded into the reactor at RT from the downstream side under a flow of 500 sccms Ar and was positioned directly above the thermocouple used to measure the heater temperature (T_H) at the centre of the 1″ QT. After closing the reactor, N_2:10% H_2 or Ar was introduced at a flow rate of 500 sccm for 5–10 min .Then the temperature was ramped to the desired growth temperature under a reduced flow of 10–500 sccm N_2:10% H_2 or Ar using rates of 10–30 °C/min. Upon reaching the growth temperature (T_G), NH_3 was introduced with a flow of 10–250 sccms for 60 min, while maintaining a constant, total flow rate, after which the tube was allowed to cool down using the same gas flows during growth. The sample was removed only when the temperature was lower than 100 °C. It should be pointed out that the 1″ QT was changed regularly in order to ensure that the interior walls in the growth zone were clean. The morphology of the GaN NWs were examined with a TESCAN scanning electron microscope (SEM) while their crystal structure and the phase purity were investigated using a SHIMADZU, XRD-6000, X-ray diffractometer with a Cu–Ka source by performing a scan of θ–2θ in the range between 10° and 80°. Finally, photoluminescence (PL) measurements were carried out using a Ti–sapphire based ultrafast laser amplifier generating 75 fs pulses at repetition rate of 250 kHz. The fundamental light at 800 nm generated by the ultrafast amplifier was frequency doubled and used as the source for an *optical parametric amplifier*, which was tuned for these experiments at 580 nm. The pulses of the OPA were frequency doubled using a BBO non-linear crystal and the ultrashort pulses at 290 nm were used to excite the GaN NWs at RT with energy of 10 μW while the PL emission was collected and analyzed through a double pass spectrometer equipped with a photomultiplier.

3. Results and discussion

We will begin by considering the growth of Ga_2O_3 NWs using APCVD. A typical image of Ga_2O_3 NWs that were obtained at T_G=900 °C under a flow of 100 sccm Ar is shown in Fig. 1. The Ga_2O_3 NWs have diameters ≤50 nm, lengths up to 10 μm and exhibited peaks in the XRD corresponding to β-Ga_2O_3 as shown in Fig. 3(b) [33]. No nanostructures were obtained for T_G < 800 °C due to the fact that Ga has a low melting point of 29.8 °C together with an unusually high boiling point of 1983 °C and high surface tension, hence a low vapor pressure even at temperatures of a few hundreds °C. The growth of β-Ga_2O_3 NWs is attributed to the reaction of Ga with residual O_2 in the reactor similar to the growth of other semiconductor oxide NWs such as SnO_2 [34] and In_2O_3 [35]. It should be pointed out that a high yield and uniform distribution of β-Ga_2O_3 NWs was obtained when the distance between the Ga and Au/Si(0 0 1) was <5 mm and the mass of Ga fragments used in the reaction varied between 0.1 and 0.3 g that led to a white-blue like deposit. Prolonging the growth time from one to two hours lead to the formation of a high yield of β-Ga_2O_3 NWs with lengths up to several tens of μm. A high yield-uniform distribution of β-Ga_2O_3 NWs was easily and reproducibly obtained on 0.7 nm Au/Si(0 0 1) while one can also observe Au NPs on their ends suggesting that they grow by the vapor liquid solid (VLS) mechanism. Before describing the growth of GaN NWs via the direct reaction of Ga with NH_3 using Ar or N_2:10%H_2 it is worthwhile pointing out that GaN NWs have been obtained by Song et al. [30] by the nitridation of β-Ga_2O_3 NWs. In addition GaN NWs with diameters of 50–100 nm have been obtained by Ai et al. [30] via the nitridation of Ga_2O_3 layers, deposited on 40 nm Ti/Si(1 1 1), at 950 °C using a flow of 500 sccms of NH_3. In this case the growth of GaN NWs was suggested to proceed via the reaction $Ga_2O + 2NH_3 \rightarrow 2GaN + H_2O + 2H_2$; no GaN NWs were obtained without Ti.

Others have deliberately included SiO_2 into Ga in order to grow GaN NWs. For instance Tang et al. [25] obtained 10–50 nm diameter GaN NWs on Al_2O_3 with Fe_2O_3 as a catalyst using 0.5 g of Ga and SiO_2 under 80 sccms of NH_3, at 950 °C. In this case the Ga was proposed to react with SiO_2 leading to the formation of Ga_2O that subsequently reacts with NH_3 to form GaN.

On the other hand, Lyu et al. [26] obtained 50–60 nm GaN NWs from Ga and GaN at 1000 °C using 500 sccms of NH_3 and NiO NPs. These exhibited a strong PL peak at 3.315 eV and a broad weak emission at 2.695 eV attributed to deep level defects. However they did not obtain any GaN NWs without NiO NPs. More importantly they stated that only amorphous products were

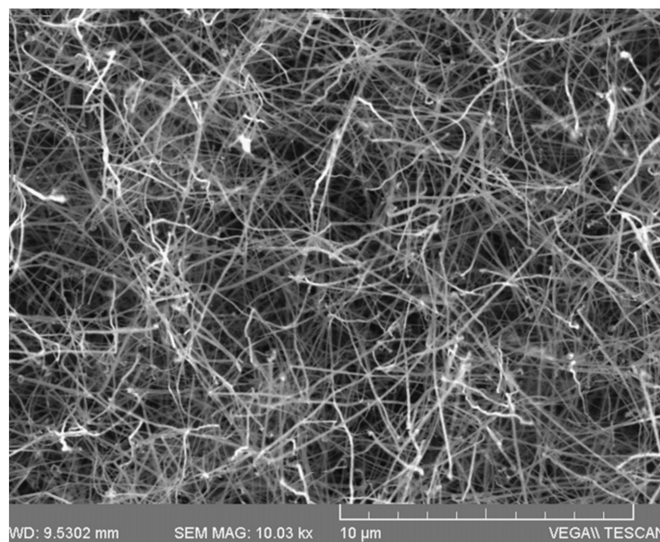

Fig.1. SEM image of Ga_2O_3 NWs obtained at T_G=900 °C under 100 sccms Ar on 0.7 nm Au/Si(0 0 1).

obtained when either Ga or GaN were individually used, similar to the findings of Narukawa et al. [36].

While the growth of GaN NWs from Ga_2O_3 may be more efficient compared to the direct nitridation of Ga the use of Ga_2O_3, SiO_2, etc and catalysts containing O_2 such as NiO, $Ni(NO_3)_2$ and Fe_2O_3 inherently leads to the incorporation of oxygen in the GaN NWs, which is not desirable since it leads to the formation of defect states in the band-gap and a deterioration in their optical and electronic properties. Therefore as stated above we carried out a detailed investigation into the growth of GaN NWs on Au/Si(0 0 1) via the direct reaction of Ga with NH_3 using either Ar or N_2:H_2 as carrier gasses under different temperatures, pressures and gas flows.

In contrast to the high yield-uniform growth of β-Ga_2O_3 NWs described above, the direct reaction of Ga with 10 sccms of NH_3 and 90 sccms of Ar at 900 °C using APCVD lead to the growth of GaN NWs on 1.1 nm Au/Si(0 0 1) and many NCs. The GaN NWs are not straight as shown in Fig. 2 and have diameters of 50 nm and lengths of a few μm's.

No improvement in the yield or shape of the GaN NWs occurred upon increasing the NH_3 flow up to 50 or even 90 sccms or by increasing the mass of Ga from 0.2 up to 0.5 g. On the other hand no deposition took place on plain Si(0 0 1). Instead the reaction of Ga with NH_3 lead predominantly to the deposition of nanocrystals (NCs) on the Au/Si(0 0 1).

At first this might seem to be consistent with the findings of Zhang et al. [18] who obtained GaN NWs only with In, Fe and Ni but not with Au. While Au NPs are effective for the growth of InP, Si and GaAs NWs they were found to be inactive in the case of GaN. In contrast transition metals such as Fe and Ni have been commonly used for the growth of GaN NWs but the main drawback of using these is contamination, which also leads to a degradation of their electronic and optical properties. Considering that Chisholm and Bristowe [37] calculated a low defect formation energy for Ni ($\approx$1.2 eV) and a higher one for Au ($\approx$4 eV) the latter remains a good choice and several have used it successfully for the growth of GaN NWs [38–42]. GaN NWs were successfully grown on 0.7 nm Au/Si(0 0 1) via the direct reaction of Ga with NH_3 at 900 °C under a flow of 25 sccm NH_3 and 75 sccms of a N_2:10% H_2 mixture, as shown in Fig. 3(a) The GaN NWs have diameters of 50 nm and lengths up to 2 μm confirming that Au does not inhibit their growth. In addition to the higher yield there is also a significant improvement in the shape of the GaN NWs that are now straight. Evidently the replacement of Ar with N_2:10% H_2 enhances the growth of GaN NWs on Au/Si(0 0 1) although their lengths are considerably smaller than that of Ga_2O_3 NWs. The GaN NWs exhibited clear peaks in the XRD as shown in Fig. 3(b), corresponding to GaN with a hexagonal wurtzite structure and lattice constants of a=0.318 nm and c=0.518 nm [25].

Excitation of the GaN NWs shown in Fig. 3(a) using ultrafast pulses of λ=290 nm resulted in strong RT PL shown in Fig. 4 where the prominent peak corresponds to band edge emission of GaN at 3.42 eV ($\equiv$362 nm). Note that there was very little luminescence around 540 nm commonly referred to as the "yellow luminescence" band of GaN. In these GaN NWs the ratio of the band edge emission to the yellow luminescence was $\approx$970:1. In addition to PL, time resolved PL were carried out using time-correlated single photon counting (TCSPC). The inset in Fig. 4 shows TCSPC PL obtained at three different emission wavelengths namely at λ=365, 400 and 450 nm over a time span of ~45 ns. Although the measured PL signal comes from a particular energy state, the non-radiative channels available to the photogenerated carriers in these states alter the population thus making the PL decay appear multi-exponential. The decay of the band edge emission at λ=365 nm appears to be dominated by a single fast component with τ=0.40 ns, see Table 1. Emission at longer wavelengths appears to have slightly longer decays corresponding

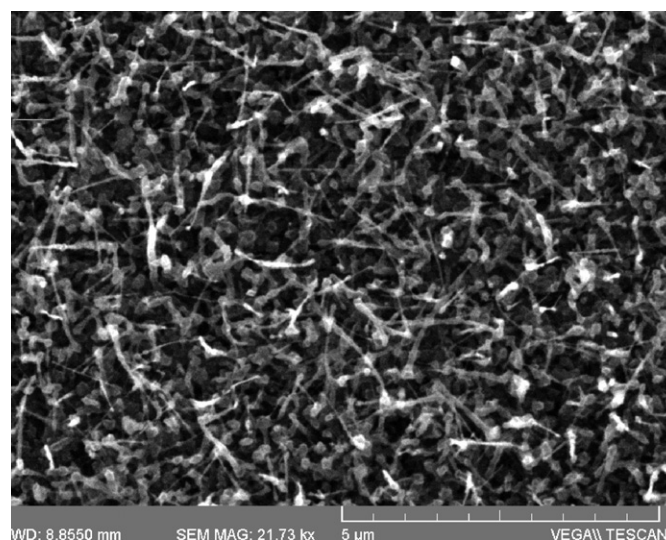

Fig.2. SEM image of the GaN NWs obtained at T_G=900 °C under 90 sccm Ar and 10 sccm NH_3 on 1.1 nm Au/Si(0 0 1). The GaN NWs are not straight and have non-uniform diameters.

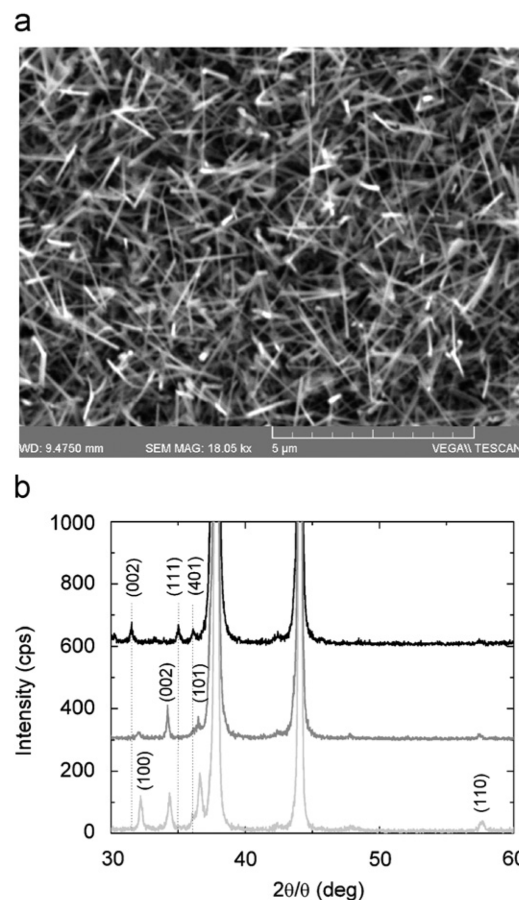

Fig.3. (a) SEM image of GaN NWs obtained at T_G=900 °C under 20 sccm NH_3 and 80 sccms N_2:10% H_2 on 0.7 nm Au/Si(0 0 1) (b) Top trace: XRD corresponding to monoclinic β-Ga_2O_3 with lattice constants a=12.23 Å, b=3.04 Å, c=5.80 Å and β=103.7° [33]; Middle (N_2: 10% H_2: NH_3) and lower (Ar) traces correspond to GaN NWs with peaks corresponding to the (1 0 0), (0 0 2), (1 0 1) crystallographic planes of the hexagonal wurtzite structure of GaN with lattice constants a=0.318 nm and c=0.518 nm [25].

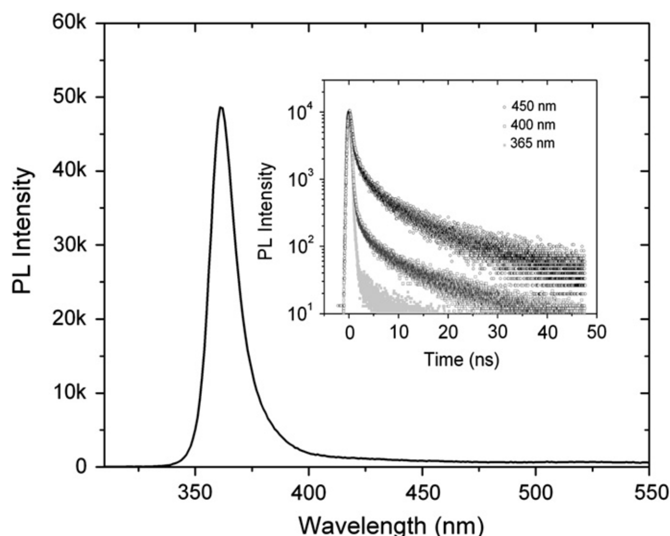

Fig.4. PL from the straight GaN NWs obtained using N_2:10% H_2. The inset shows TCSPC PL from the GaN NWs excited with an ultrafast laser pulse at 290 nm and probed at 365, 400 and 450 nm.

Table 1
Time constants obtained from a tri-exponential fir of $I(t)=\alpha_1 e_1^{-t/\tau}+\alpha_2 e_2^{-t/\tau}+\alpha_3 \exp_3^{-t/\tau}$ to the decays of Fig. 4.

n	$\lambda=365$ nm		$\lambda=400$ nm		$\lambda=450$ nm	
	τ_n(ns)	α_n(%)	τ_n(ns)	α_n(%)	τ_n(ns)	α_n(%)
1	0.40	99.9	0.44	99	0.62	86
2	23.7	0.1	15.4	1	4.67	11
3	–	–	–	–	22.6	3

to energy states below the band edge which are described well only by a tri-exponential decay.

In an attempt to improve the yield and increase the length of the GaN NWs the reaction of Ga with NH_3 was carried out at low pressure in order to eliminate oxygen also. Initially, the reaction of 0.4 g of Ga with 25 sccm of NH_3/75 sccms Ar at 950 °C under 1.5 Torr lead to the deposition of Ga drops as large as 25 μm and a few ultra long GaN NWs protruding from their surface. These are similar those of He et al. [43], who obtained GaN NWs with diameters between 26 and 100 nm and lengths up to 500 μm via the direct reaction of 3 g of Ga with 50–100 sccms NH_3 at 15 Torr and 900 °C. Their GaN NWs formed a network on top of an amorphous matrix of GaN, no catalyst was employed and the yield of GaN NWs was rather low, similar to what we obtained. Smaller amounts of Ga were subsequently used to avoid the formation of large drops and an underlying layer of crystals. However the reaction of 50 mg of Ga with 10 sccm NH_3:90 sccms Ar during the growth step at 900 °C under 1.2 Torr still lead to the deposition of crystals and droplets as large as 10 μm but no GaN NWs. However a uniform thin layer consisting of 0.5 μm long hexagonal GaN rods with diameters of 200 nm were obtained at 800 °C while lower temperatures favored the deposition of a uniform layer of close packed NPs under pressures of a few Torr, see Table 2. It should be noted that no GaN NWs were obtained by varying the NH_3 gas flow between 10 and 200 sccm NH_3 or by using N_2:10% H_2 at pressures of a few Torr. A high yield, uniform distribution of GaN NWs was obtained by increasing the pressure above 10 Torr, using even less Ga i.e. 10–30 mg and maintaining a distance of >5 mm between the Ga and Au/Si(0 0 1). This lead to the growth of GaN NWs as shown in Fig. 5. The diameter of the

Table 2
GaN grown at $T_G=500$–800 °C and 2.2 Torr via the reaction of Ga with 100 sccms of NH_3 alone, using 100 sccms of Ar during the temperature ramp with $dT/dt=10$ °C/min. A larger quantity of Ga was used at $T_G=500$ °C in order to maintain the Ga vapor pressure above the Au/Si(0 0 1) surface but no deposition occurred.

CVD525	800 °C	75 mg	1.0 nm Au	0.5 μm long hexagonal rods
CVD526	700 °C	88 mg	1.0 nm Au	Close packed NPs uniform
CVD527	600 °C	88 mg	1.0 nm Au	Close packed NPs uniform
CVD528	500 °C	184 mg	0.7 nm Au	No deposits

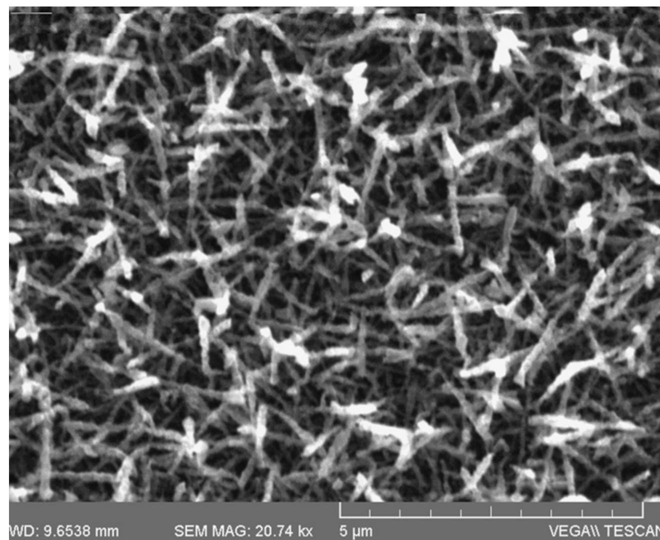

Fig.5. SEM image of GaN NWs with rough surfaces obtained from the reaction of 18 mg Ga with 10 sccms of NH_3 and 115 sccms of Ar at $T_G=950$ °C and $P=8$ Torr.

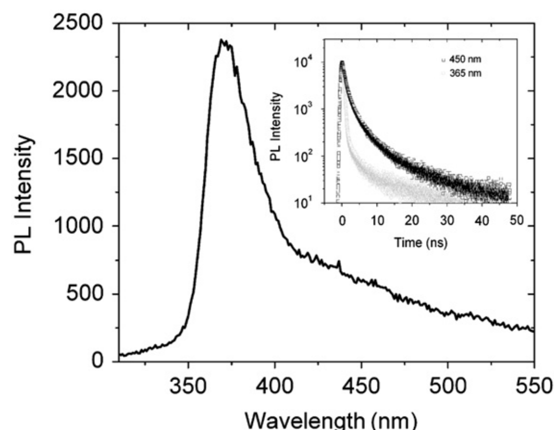

Fig.6. PL spectrum of GaN NWs exhibiting near band edge emission at 3.42 eV and 'yellow' broadband emission. The inset shows TCSPC PL at $\lambda=365$ and 450 nm using an ultrafast laser pulse at 290 nm.

GaN NWs is 50 nm with lengths reaching up to 3 μm while there was a clear tendency for the formation of such GaN NWs using pressures over the entire range between 10 and 100 Torr and using a few tens of sccms of NH_3 and Ar at $T_G=950$ °C. It should be noted again that changing the flow of NH_3 did not lead to the growth of straight, uniform diameter GaN NWs. The GaN NWs shown in Fig. 5 also exhibited clear peaks in the XRD corresponding to hexagonal wurtzite GaN while RT PL is shown in Fig. 6.

Before considering the PL of these GaN NWs it is worthwhile pointing out that a systematic investigation into the growth of

Table 3
Time constants obtained from a tri-exponential fit of $I(t)=\alpha_1 e_1^{-t/\tau}+\alpha_2 e_2^{-t/\tau}+\alpha_3 \exp_3^{-t/\tau}$ to the decays of Fig. 6.

n	λ=365 nm		λ=400 nm		λ=450 nm	
	τ_n(ns)	α_n(%)	τ_n(ns)	α_n(%)	τ_n(ns)	α_n(%)
1	0.51	99.6	–	–	0.91	84
2	20.1	0.4	–	–	4.09	15
3	–	–	–	–	25.6	1

GaN NWs via the reaction of Ga with NH_3:Ar at 4.5 mBar, between 800 and 1000 °C was carried out by Cai et al. [19] who used Ni, Au and $Ni(NO_3)_2$ catalysts on Si. GaN NWs were obtained using Au or Ni, only at 950 °C with 100 mg of Ga. On the other hand SiO_x NWs were grown using $Ni(NO_3)_2$. Low flow rates resulted into lower coverage and shorter GaN NWs while higher NH_3 flow rates lead to the growth of nanocrystals (NCs) in addition to GaN NWs [19].

The formation of GaN NWs at LPs < 10 Torr is most likely suppresed by the excessive Ga vapor pressure over the Au/Si(0 0 1), which is significant even at temperatures as low as 600 °C. Therefore, the growth of GaN NWs at LPs in the range 10–100 Torr occurs due to the lower Ga vapor pressure over Au/Si(0 0 1) that allows the initiation of 1D GaN NW growth. Considering that GaN NWs are obtained for $T \geq 900$ °C the successful growth of GaN NWs depends critically on the temperature, pressure and gas flows in decreasing order of importance but also the availability of reactive species which are necessary to instigate 1D NW growth.

Interestingly, the PL intensity of these GaN NWs is significantly lower compared to the PL of the straight GaN NWs seen in Fig. 4. Furthermore, the band edge emission is broader and red shifted to 3.35 eV (≡370 nm) whereas a relatively strong emission is present at longer wavelengths extending down to 550 nm. The longer wavelength emission and the observed reduction in the band edge emission is attributed to the plethora of surface and structural defect related states generated during the growth of these NWs. TCSPC PL decay curves are also shown in the inset of Fig. 6. The behavior and time constants listed in Table 3 are similar to those seen for the straight NWs in the inset of Fig. 4.

The different PL obtained from the straight GaN NWs shown in Fig. 3 and the corrugated GaN NWs of Fig. 5 are very similar to the findings of Li et al. [44] who obtained a mix of straight and zig-zag GaN NWs with diameters of 60–150 nm on 10 nm Au/6H–SiC via the reaction of Ga with 20 sccms NH_3 at 850 °C The straight GaN NWs exhibited near, band edge PL in contrast to the zig-zag GaN NWs which exhibited only broad, yellow, PL which was attributed to O_2 and N vacancies. Similar PL was obtained from GaN NWs with diameters of 10–50 nm grown by Chen et al. [23] on Si(0 0 1) by the direct reaction of Ga with 18 sccms NH_3 at 910 °C using a mixture of In, Fe, Ni and Co catalysts. The PL spectrum exhibited strong band edge emission at 3.4 eV and broad PL around 2.3 eV corresponding to yellow luminescence.

From the above it is evident that the growth conditions are critical in obtaining high quality, straight GaN NWs with good optical and electronic properties. However this may be achieved only by understanding the growth mechanisms in detail.

The most commonly invoked mechanism on the growth of GaN NWs is the VLS mechanism whereby the Ga and N enter the catalyst NP and lead to the formation of GaN NWs as shown in Fig. 7(a). However a more careful analysis of the relation between the radii of the Au NP and GaN NWs, carried out by Kuo et al. [21], led them to propose an alternative mechanism whereby the Ga enters the Au NP which sits on top of the GaN NW and forms an Au–Ga alloy but Ga also reacts with N at the top of the GaN NW outside and away from the Au NP. To be specific they obtained GaN NWs from the reaction of Ga with 10 sccms NH_3 at 920 °C on Si using Au NPs with a very narrow distribution of sizes. The GaN NWs had diameters at least twice as large as the Au NPs and a simple model was put forward accounting for the stable growth of GaN NWs where the radius of the Au NP is smaller than the radius of the GaN NW. In addition it was argued that Au NPs with diameters equal to or larger than the GaN NWs do not favor stable growth. This is somewhat similar to the mechanism for the spontaneous growth of GaN nanowires by MBE which has been described in detail by Bertness et al. [15]. Ga atoms that impinge on the nanowire tip or within a surface diffusion length of the tip will incorporate. Adatoms arriving farther down the sides are likely to desorb rather than incorporate and the GaN is shown growing out of a GaN matrix layer. Concerning GaN NWs, there is general agreement on the fact that their steady-state growth regime is governed by Ga diffusion up to the top of existing wires but the nucleation process and the subsequent transient regime are, to some extent, a matter of controversy [14].

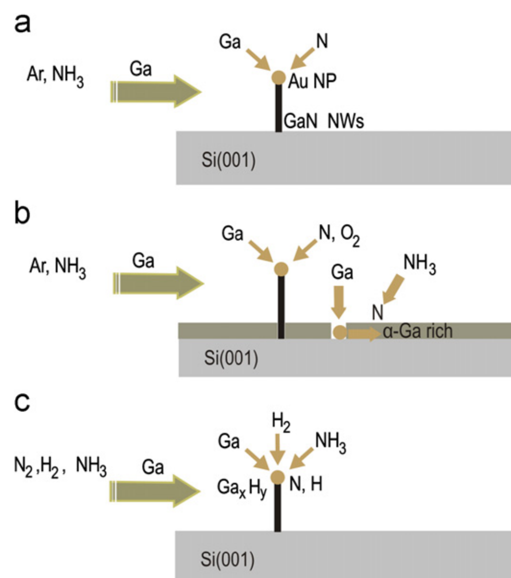

Fig.7. Schematic diagrams for (a) commonly invoked mechanism for the growth of GaN NWs obtained from the reaction of Ga with N via the VLS mechanism (b) Preferential formation of an amorphous Ga rich oxynitride layer from the direct reaction of Ga with NH_3 under Ar (c) GaN NWs obtained using N_2:H_2 as opposed to Ar.

Now as already described above the reaction of Ga with residual O_2 under a flow of Ar leads to a high yield growth of Ga_2O_3 NWs on Au/Si(0 0 1). In this case Au NPs absorb Ga until they become supersaturated after which β-Ga_2O_3 NW growth commences due to the efficient oxidation of Ga. Gold NPs do not react with oxygen and therefore keep absorbing Ga from the main gas stream leading to the formation of Ga_2O_3 NWs with lengths up to tens of μm via the VLS mechanism. In contrast the reaction of Ga with NH_3 under a flow of Ar lead to a lower yield of bent GaN NWs on top of an amorphous α-layer. As stated above the low or zero yield of GaN NWs obtained from the direct reaction of Ga with NH_3 on Au/Si(0 0 1) is usually attributed to the poor solubility of N in Au which is thought to lead to a suppression of the VLS mechanism. However before elaborating further it is worthwhile pointing out that the partial decomposition of NH_3 and the production of reactive N at elevated temperatures is limited. In addition the catalytic decomposition of NH_3 over different metals has been investigated in detail and a comparison showed that decomposition is effective in the following order: Ru > Ni > Rh > Co > Ir > Fe ≫ Pt > Cr > Pd > Cu ≫ Te [48]. While

NH_3 does not dissociate over Au [49] it is known to dissociate on Si(0 0 1) which may be the reason behind the preferential formation of the Ga rich layer [50]. However as already described above no deposition occurred on plain Si(0 0 1). Therefore it is very likely that Ga is absorbed at the Au NPs sites leading to the formation of a Ga rich α-layer as shown in Fig. 7(b). The low yield and limited length of GaN NWs compared to that of β-Ga_2O_3 NWs is due to the limited reactivity and availability of elemental Ga and N at the Au NP sites while their bent appearance is probably due to strain produced by the formation of β-Ga_2O_3. In this case the 1D growth may be actually instigated by the reaction of Ga with O_2. Note that the formation of the α-Ga rich oxynitride layer, shown schematically in Fig. 7(b), is not likely related to the large size of the Au NPs for otherwise we would have not obtained β-Ga_2O_3 NWs and straight GaN NWs under H_2. The growth of higher quality GaN NWs via the direct reaction of Ga with NH_3 was achieved by the use of N_2:10% H_2 as opposed to Ar which first of all eliminates O_2. Furthermore the H_2 dissociates into H at the Au NP sites and reacts with Ga forming Ga_xH_y [45]. It has been shown for that the formation energy of GaH_2 is lower than that of elemental Ga in the temperature range 800–1000 °C [46] so it is very likely that reactive Ga_xH_y will form at 900 °C. The formation of reactive Ga_xH_y gas in the vicinity of the Au NPs promotes the growth via its reaction with dissociated NH_3 [47] at the tops of the GaN NWs as shown in Fig. 7(c). Moreover the formation of the α-Ga rich layer is suppressed since the Ga reacts with H in the vicinity of the Au NP leading to the production of Ga_xH_y which is a gas. The limited length of the GaN NWs ($\approx$ 2–3 μm) obtained under Ar:NH_3 but also N_2:10% H_2:NH_3 compared to the large length of β-Ga_2O_3 NWs ($\approx$ 10 μm) is most likely due to the lower concentration of reactive species. Further work is however necessary to clarify in greater detail the growth mechanisms and the chemistry involved.

4. Conclusions

High quality, straight GaN nanowires with diameters of 50 nm and lengths of 3 μm have been grown by hydride-assisted chemical vapor deposition on Au/Si(0 0 1) via the reaction of Ga with NH_3 and H_2 at 900 °C. These exhibited intense, near band edge PL at 3.4 eV in contrast to bent GaN NWs with non-uniform diameters obtained with Ar and NH_3 which were found to have a broadband yellow emission related to surface, structural imperfections.

A growth mechanism has been proposed whereby one-dimensional (1D) growth is promoted by the catalytic action of Au NPs that leads to the dissociation of H_2 its reaction with Ga and the preferential formation of Ga_xH_y which reacts efficiently with dissociated NH_3 at the top of the GaN NWs while suppressing at the same time the formation of an amorphous Ga rich layer. Consequently Au NPs act catalytically in favor of the growth of high quality GaN NWs in conjunction with H_2 which is important for the realization of nanoscale electronic and optoelectronic devices.

Acknowledgment

The work in this article was supported by the *Research Promotion Foundation of Cyprus* under grant BE0308/03, for fundamental research in the area of nanotechnology.

References

[1] S. Seo, G.Y. Zhao, D. Pavlidis, Electron. Lett. 44 (2008) 244.
[2] Y. Taniyasu, M. Kasu, T. Makimoto, Nature 441 (2006) 325.
[3] S. Nakamura, T. Mukai, M. Sengh, Appl. Phys. Lett. 64 (1994) 1687.
[4] J. Wu, W. Walukiewicz, K.M. Yu, J.W. Ager, et al., Appl. Phys. Lett. 80 (2002) 3967.
[5] Properties of advanced semiconductor materials: GaN, AlN, InN 0471358274.
[6] J. Li, K.B. Nam, M.L. Nakarmi, J.Y. Lin, et al., Appl. Phys. Lett. 83 (2003) 5163.
[7] M. Zervos, A. Kostopoulos, G. Constantinidis, et al., J. Appl. Phys. 91 (2001) 4387.
[8] E. Iliopoulos, A. Georgakilas, E. Dimakis, et al., Phys. Status Solidi 203 (2006) 102.
[9] A. Othonos, M. Zervos, M. Pervolaraki, Nanoscale Res. Lett. 4 (2009) 122.
[10] C.K. Kuo, C.W. Hsu, C.T. Wu, Z.H. Lan, C.Y. Mou, et al., Nanotechnology 17 (2006) 332.
[11] J. Su, G. Cui, M. Gherasimova, H. Tsukamoto, et al., Appl. Phys. Lett. 86 (2005) 013105.
[12] T. Kuykendall, P. Ulrich, S. Aloni, P. Yang, Nat. Mater. 6 (2007) 1961.
[13] T. Kuykendall, P.J. Pauzauskie, S. Lee, Y.F. Zhang, et al., Nano Lett. 3 (2003) 1063.
[14] T. Stoica, E. Sutter, R.J. Meijers, R.K. Debnath, R. Calarco, et al., Small (2008).
[15] K.A. Bertness, A. Roshko, L.M. Mansfield, et al., J. Cryst. Growth 310 (2008) 3154.
[16] M. He, I. Minus, P. Zhou, S.N. Mohammed, et al., Appl. Phys. Lett. 77 (2000) 3731.
[17] J.C. Wang, S.Q. Feng, D.P. Yu, Appl. Phys. A 75 (2002) 691.
[18] J. Zhang, L. Zhang, J. Vac. Sci. Technol. B 21 (2003) 2415.
[19] X.M. Cai, A.B. Djurisic, M.H. Xie, et al., Appl. Phys. Lett. 87 (2005) 183103.
[20] B. Ha, S.H. Seo, J.H. Cho, C.S. Yoon, J. Yoo, et al., J. Phys. Chem. 109 (2005) 11095.
[21] C.K. Kuo, C.W. Hsu, C.T. Wu, Z.H. Lan, C.Y. Mou, et al., Nanotechnology 17 (2006) 332.
[22] X.M. Cai, A.B. Djurisic, M.H. Xie, S. Gwo, et al., Thin Solid Films 515 (2006) 984.
[23] C.C. Chen, C.C. Yeh, C.H. Chen, M.Y. Yu, et al., J. Am. Chem. Soc. 123 (2001) 2791.
[24] P.G. Li, X. Guo, X. Wang, W.H. Tang, J. Alloys Compd. 475 (2009) 463.
[25] C.C. Tang, S.S. Fan, H.Y. Dang, P. Li, et al., Appl. Phys. Lett. 77 (2000) 1961.
[26] S.C. Lyu, O.H. Cha, E.-K. Suh, H. Ruh, et al., Chem. Phys. Lett. 367 (2003) 136.
[27] A.B. Djurišić, K.H. Tam, Y.F. Hsu, S.L. Zhang, et al., Thin Solid Films 516 (2007) 238.
[28] L. Yu, Y. Ma, Z. Hu, J. Cryst. Growth 310 (2008) 5237.
[29] K.-W. Chang, J.J. Wu, J. Phys. Chem. B 106 (2002) 7796.
[30] Y. Ai, C. Xue, C. Sun, L. Sun, H. Zhuang, F. Wang, et al., Mater. Lett. 61 (2007) 2833;
Y.P. Song, H.Z. Zhang, C. Lin, W. Zhu, G.H. Li, F.H. Yang, et al., Phys. Rev. B 69 (2004) 075304.
[31] H.Z. Zhang, B. Li, Li, C.S Xue, et al., Microelectron. J. 39 (2008) 1629.
[32] W. Lv, L. Wu, Y. Wu, R. Xv, H. Gai, K. Zou, J. Cryst. Growth 302 (2007) 1.
[33] C.L. Kuo, M.H. Huang, Nanotechnology 19 (2008) 155604.
[34] A. Othonos, M. Zervos, D. Tsokkou, Nanoscale Res. Lett. 4 (2009) 828.
[35] D. Tsokou, M. Zervos, A. Othonos, J. Appl. Phys. 106 (2009) 084307.
[36] M. Narukawa, S. Koide, H. Miyak, K. Hiramatsu, J. Cryst. Growth 311 (2009) 2970.
[37] J.A. Chisholm, P.D. Bristowe, Comp. Mat. Sci 22 (2001) 73.
[38] A. Chatterjee, S. Chattopadhyah, C.W. Hsu, C.H. Shen, et al., J. Mater. Res. 19 (2004) 1768.
[39] S. Dhara, A. Datta, C.T. Wu, Z.H. Lan, K.H. Chen, et al., Appl. Phys. Lett. 82 (2003) 451.
[40] S.K. Lee, H.K. Choi, P. Pauzauskie, P.D. Yang, et al., Phys. Status Solidi B 241 (2004) 2775.
[41] C. Cao, X. Xiang, H. Zhu, J. Cryst. Growth 273 (2005) 375.
[42] Z. Yu, Z. Yang, S. wang, Y. Jin, J.G. Liu, et al., Chem. Vapor. Dep. 11 (2005) 433.
[43] M. He, I. Minus, P. Zhou, S.N. Mohammed, et al., Appl. Phys.Lett. 77 (2000) 3731.
[44] P.G. Li, X. Guo, X. Wang, W.H. Tang, J. Alloys Compd. 475 (2009) 463.
[45] T. Fujitani, I. Nakamura, T. Akita, et al., Angew. Chem. Int. Ed. 48 (2009) 9515–9518;
E. Bus, J.T. Miller, J.A. van Bokhoven, J. Phys. Chem. B 109 (2005) 14581.
[46] F. Kawamura, M. Imade, M. Yoshimura, Y. Mori, et al., Jpn. J. Appl. Phys. 44 (2005) 1.
[47] W.C. Hou, F.C.-N. Hong, Nanotechnology 20 (2009) 055606.
[48] J.C. Ganley, F.S. Thomas, E.G. Seebauer, R.I. Masel, Catal. Lett. 96 (2004) 117.
[49] J. Gong, R.A. Ojifinni, T.S. Kim, et al., J. Am. Chem. Soc. 128 (2006) 9012.
[50] F. Bozso, Ph. Avouris, Phys. Rev. Lett. 57 (1986) 1185;
R.P. Hamers, Ph. Avouris, F. Bozso, Phys. Rev. Lett. 59 (1987) 2071;
F. Bozso, Ph. Avouris, Phys. Rev. B 38 (1988) 3937.